

Article

Construction of a Bacterial Lipidomics Analytical Platform: Pilot Validation with Bovine Paratuberculosis Serum

Paul L. Wood ^{1,*}  and Erdal Erol ²

¹ Metabolomics Unit, College of Veterinary Medicine, Lincoln Memorial University, 6965 Cumberland Gap Pkwy, Harrogate, TN 37752, USA

² Department of Veterinary Science, Veterinary Diagnostic Laboratory, University of Kentucky, Lexington, KY 40546, USA; erdal.erol@uky.edu

* Correspondence: paul.wood@lmunet.edu

Abstract: Lipidomics analyses of bacteria offer the potential to detect and monitor infections in a host since many bacterial lipids are not present in mammals. To evaluate this omics approach, we first built a database of bacterial lipids for representative Gram-positive and Gram-negative bacteria. Our lipidomics analysis of the reference bacteria involved high-resolution mass spectrometry and electrospray ionization with less than a 1.0 ppm mass error. The lipidomics profiles of bacterial cultures clearly distinguished between Gram-positive and Gram-negative bacteria. In the case of bovine paratuberculosis (PTB) serum, we monitored two unique bacterial lipids that we also monitored in *Mycobacterium avian* subspecies *PTB*. These were PDIM-B C82, a phthiodiolone dimycoserolate, and the trehalose monomycolate hTMM 28:1, constituents of the bacterial cell envelope in mycolic-containing bacteria. The next step will be to determine if lipidomics can detect subclinical PTB infections which can last 2-to-4 years in bovine PTB. Our data further suggest that it will be worthwhile to continue building our bacterial lipidomics database and investigate the further utility of this approach in other infections of veterinary and human clinical interest.

Keywords: bacterial lipidomics; bovine paratuberculosis; mycolic acids; lipoteichoic acids; high-resolution mass spectrometry



Citation: Wood, P.L.; Erol, E.

Construction of a Bacterial Lipidomics Analytical Platform: Pilot Validation with Bovine Paratuberculosis Serum. *Metabolites* **2023**, *13*, 809. <https://doi.org/10.3390/metabo13070809>

Academic Editor: Harald C. Köfeler

Received: 16 May 2023

Revised: 23 June 2023

Accepted: 27 June 2023

Published: 29 June 2023



Copyright: © 2023 by the authors. Licensee MDPI, Basel, Switzerland. This article is an open access article distributed under the terms and conditions of the Creative Commons Attribution (CC BY) license (<https://creativecommons.org/licenses/by/4.0/>).

1. Introduction

Lipidomics is a rapidly evolving “omics” platform that provides valuable information regarding structural, energy source/reserve, and signal-transduction lipid pools. Bacteria possess a number of unique lipids that are not present in their mammalian hosts. This provides the opportunity of lipidomics to obtain valuable non-mammalian lipid data that can (i) detect bacterial infection in a host, (ii) monitor the progression of an infection, (iii) monitor the efficacy of treatments on an infection, and (iv) potentially define new targets in the design of targeted antimicrobial therapeutics.

While the individual lipids of a given lipid family for a bacterial strain will alter with development and with environmental stresses, lipid families will be preserved and can be monitored. Our first high-level overview is a comparison of our current knowledge base for Gram-positive vs. Gram-negative bacterial lipidomics.

1.1. Gram-Positive Bacteria

1.1.1. Gram-Positive Bacteria: Lipoteichoic Acids

Gram-positive bacteria possess a cytoplasmic membrane and a multilaminar cell wall [1]. Between the cell membrane and cell wall is a heteropolysaccharide meshwork of peptidoglycans and arabinogalactans. Teichoic acids, which anchor to peptidoglycans in the cell wall, and lipoteichoic acids (LTAs), which are found in the cell membrane, are lipids that are unique to Gram-positive bacteria, providing a strong negative charge to the cell

wall [2]. Precursors to LTAs that have been monitored in Gram-positive bacteria include a number of glycolipids (Table 1).

Table 1. Gram-positive bacterial lipoteichoic-acid-associated lipids.

Lipid Class	Bacterial Strains	References
Mono-hexosyl-monoacylglycerol (MHMG)	<i>S. mitis</i> and <i>S. oralis</i> , <i>C. cadaveris</i> , <i>C. fallax</i>	[3–5]
Dihexosyl-MG (DHMG)	<i>S. pneumoniae</i> , <i>S. mitis</i> , <i>S. oralis</i> , <i>S. mutans</i>	[4,6]
Mono-hexosyl-diacylglycerol (MHDG)	<i>S. pneumoniae</i> , <i>S. mitis</i> , <i>S. oralis</i> , <i>C. fallax</i> , <i>S. mutans</i> , <i>Rhomboutsia</i> spp., <i>B. licheniformis</i> , <i>Clostridia</i> spp., <i>L. johnsonii</i>	[4–10]
DHDG	<i>S. mitis</i> and <i>S. oralis</i> , <i>C. fallax</i> , <i>S. mutans</i> , <i>Rhomboutsia</i> spp., <i>B. licheniformis</i> , <i>Clostridia</i> spp., <i>L. johnsonii</i>	[4–10]
Lipoteichoic Acid Primer (LTAP; DHDG-GroP)	<i>Streptococcus</i> spp., <i>B. licheniformis</i> , <i>Clostridia</i> spp., <i>Listeria</i> spp., <i>Bacillus subtilis</i>	[4–6,8,9,11]
Alanylated-LTAP (LTAP-Ala) and Di-Alanylated-LTAP	<i>Bacillus licheniformis</i> , <i>Bacillus subtilis</i>	[8,12,13]
Diglycerophosphate-DHDG (LTAdiP)	<i>S. pneumoniae</i> , <i>S. mitis</i> , <i>S. oralis</i> , <i>Listeria</i> spp.	[4,14]
Tri- and Tetra-Hexosyl-DG	<i>Rhomboutsia</i> spp., <i>Clostridia</i> spp.	[7,9]
Ala-DG	<i>Bacillus subtilis</i> , <i>Corynebacterium glutamicum</i>	[12,15–17]
Glucuronosyl-DG (GlcA-DG)	<i>Corynebacterium glutamicum</i>	[16–18]
Lysyl-DG and Lysyl-Galactosyl-DG	<i>Staphylococcus</i> spp.	[19,20]
Mannosyl-Glucuronosyl-DG (Man-GlcA-DG)	<i>Corynebacterium glutamicum</i> , <i>C. striatum</i>	[16–18]
N-Acetylglucosamine-DG (GlcNAc-DG)	<i>Clostridia</i> spp.	[9,19]
Phosphoethanolamine-GlcNAc-DG (PE-GlcNAc-DG)	<i>Clostridia</i> spp.	[9,21]
PE-MHDG and PE-DHDG	<i>Clostridia</i> spp.	[9,21]
Type IV LTA intermediates	Oral commensal bacteria	[4]

The diversity of LTA precursor lipidomes between different bacterial species is demonstrated by the detection of DHMG in only 12 of 19 clostridia species examined [9]. The further modification of these lipids through the addition of phosphoethanolamine only was present in 4 of those 12 species [9].

1.1.2. Gram-Positive Bacteria: Modified Phosphatidylglycerols

Aminoacylation of phosphatidylglycerol (PG) is another unique feature in the lipidome of Gram-positive bacteria (Table 2). The pathway for these aminoacylations is phosphatidic acid → CDP-DG → phosphatidylglycerophosphate → PG → aminoacyl-PG.

Table 2. Gram-positive bacterial aminoacyl phosphatidylglycerols (PGs).

Lipid Class	Bacterial Strains	References
Precursor CDP-DG	<i>Corynebacterium glutamicum</i> , <i>C. striatum</i> , <i>Clostridia</i> spp.	[16–18,22]
Lysyl-PG	<i>Bacillus</i> spp., <i>Clostridium</i> spp., <i>Lactobacillus</i> spp., <i>Staphylococcus</i> spp.	[23,24]
Alanyl-PG	<i>P. aeruginosa</i> , <i>Clostridia</i> spp., <i>Bifidobacteria</i> spp., <i>Staphylococci</i> spp., <i>Listeria</i> spp., <i>Bacillus</i> spp., <i>C. Corynebacterium</i> , <i>B. subtilis</i>	[12,13,15,16,23,24]

Table 2. Cont.

Lipid Class	Bacterial Strains	References
Leucyl-PG	<i>B. subtilis</i>	[12,13]
Succinyl-Lysyl-PG	<i>B. subtilis</i>	[12,25]
Arginyl-PG	<i>Enterococcus</i> spp., <i>Staphylococci</i> spp., <i>Listeria</i> spp., <i>Bacillus</i> spp.	[23,24]
Ornithinyl-PG	<i>Bacillus</i> , <i>Mycobacteria</i> spp	[23,24,26]
Aspartyl-PG	<i>B. subtilis</i>	[12,13]

The diversity of amino acyl lipidomes between different bacterial species is demonstrated by the detection of lysyl-PG in only 5 of 24 clostridia species examined [9] and the detection of alanyl-PG in only 3 of 24 clostridia species examined [9].

1.1.3. Gram-Positive Bacteria: Mycolic Acids

A very unique family of glycolipids is also present in the outer wall of a number of bacteria in the Actinomycetes taxonomic group. These are the mycolic acids present in mycolic-acid-containing bacteria (MACB) [1,27] which include *Mycobacteria* (*M. tuberculosis*, *M. leprae*, *M. bovis*, *Tskamurella pulmonis*, *Rhodococcus erythropolis*, *R. opacus*, and *R. equi*) and *Corynebacteria* (*C. glutamicum*) [27,28]. Long-chain mycolic acids are covalently bound in the inner layer of the cell wall but are present as free acids in the outer domain. Lipids in this lipid family are diverse (Table 3).

Table 3. Gram-positive bacterial mycolic acids.

Lipid Class	Bacterial Strains	References
Mycolic acids (C76–C88; α -, keto-, and methoxy)	<i>M. tuberculosis</i>	[29,30]
Mycolic acids (C30-46)	<i>R. equi</i>	[31]
TMM (Trehalose MonoMycolates: hydroxy, keto, acetyl)	<i>Corynebacterium glutamicum</i> , <i>C. striatum</i> , <i>R. equi</i>	[16–18,32]
Acyl-TMM (Mycolic-Acyl-Trehalose)	<i>Corynebacterium glutamicum</i> , <i>C. striatum</i>	[18]
TDM (Trehalose dimycolate)	<i>Corynebacterium glutamicum</i> , <i>C. striatum</i>	[18]
Acyltrehalose (MAT) and Diacyltrehalose (DAT)	<i>Rhodococcus ruber</i> , <i>M. tuberculosis</i>	[33,34]
Acyl- and Diacyl-Sulfotrehalose	<i>Rhodococcus ruber</i> , <i>M. tuberculosis</i>	[33,35–37]
Mycolic acid-PG (1-Mycolic-2-16:0 PG)	<i>Corynebacterium glutamicum</i> , <i>C. striatum</i>	[18]
Phthiocerol (methoxy, DIMA) / Phthiodiolone (keto, DIMB) Dimycocerosates	<i>Mycobacteria</i> spp.	[38,39]

1.1.4. Gram-Positive Bacteria: Mannosyl Phosphoinositols (PIMs)

PIMs are unique to *Mycobacteria* (*M. tuberculosis*, *M. leprae*, *M. bovis*, *Tskamurella pulmonis*, *Rhodococcus erythropolis*, and *R. opacus*, *R. equi*) and *Corynebacteria* (*C. glutamicum*) [27–29] (Table 4). They are critical structural components of both the outer and inner membranes of the cell envelope.

Table 4. Gram-positive bacterial mannosyl phosphoinositols (PIs).

Lipid Class	Bacterial Strains	References
PIM1 (mannosyl-PI), PIM2 (dimannosyl-PI)	<i>Mycobacteria</i> spp., <i>Streptomyces coelicolor</i> , <i>Nocardia</i> spp., <i>Corynebacteria</i> spp.	[1,38–42]
Acyl-PIM2	<i>Mycobacteria</i> , <i>Corynebacteria</i>	[16,35–41]

1.1.5. Gram-Positive Bacteria: Aminoacyl Lipids

While bacteria possess low levels of choline (PC) and ethanolamine (PE) glycerophospholipids, a number of aminoacylated forms of these lipids are present in the membranes of Gram-positive bacteria (Table 5).

Table 5. Gram-positive bacterial aminoacyl phosphatidylethanolamines (PEs).

Lipid Class	Bacterial Strains	References
Alanyl-PE	<i>Bacillus subtilis</i>	[13]
Lysyl-PE	<i>Bacillus subtilis</i>	[13]
PE Glycerol Acetals	<i>Clostridium fallax</i> but not <i>C. cadaveris</i>	[43–45]
GPCR Ligands	Oral Commensal bacteria	[5,9]

1.2. Gram-Negative Bacteria

1.2.1. Gram-Negative Bacteria: Glycosyl Hydroxy Fatty Acids (HFAs) and Glycosyl-FAHFAs

Gram-negative bacteria possess a cell envelope comprising an inner and outer membrane with an intermediate peptidoglycan layer. Lipid A is a major membrane lipid in Gram-negative bacteria. This complex lipid has a core scaffold of P-glucosamine-glucosamine with acyl or FAHFA substitutions of the nitrogen in each hexose and acyl substitution of the hydroxy group in P-glucosamine [46–48].

Fatty acyls of hydroxy fatty acids (FAHFAs) [49] are present at high concentrations in Gram-negative bacteria, and both the glycosylated and aminoacyl forms are critical membrane constituents. The glycosylation of hydroxy fatty acids yields rhamnolipids, which act as biosurfactant antimicrobials. Representative glycolipids in Gram-negative bacteria are presented in Table 6.

Table 6. Gram-negative bacterial glycosyl hydroxy fatty acids (HFAs) and fatty acyls of hydroxy fatty acids (FAHFAs).

Lipid Class	Bacterial Strains	References
Lipid A variants	<i>P. aeruginosa</i> , <i>E. coli</i>	[45–48]
Rhamnosyl- and Di-Rhamnosyl-3-HFA	<i>Pseudomonas</i> spp., <i>Actinobacter calcoaceticus</i> , <i>Enterobacter asburiae</i>	[50–54]
Isopentyl metabolites	<i>Francisella novicida</i>	[55,56]
Menaquinones (MK-7, MK-8, and MK-9)	<i>Rhodococcus</i> spp., <i>Mycobacterium</i> spp., <i>Nocardia</i> spp.	[57]

1.2.2. Gram-Negative Bacteria: Aminoacyl Hydroxy Fatty Acids (HFAs) and FAHFAs

Gram-negative bacteria possess a diverse array of aminoacyl HFAs and FAHFAs that serve as virulence factors (Table 7).

Table 7. Gram-negative bacterial aminoacyl hydroxy fatty acids (HFAs) and fatty acyls of hydroxy fatty acids (FAHFAs).

Lipid Class	Bacterial Strains	References
Gly-FAHFA	<i>Bacteroidetes</i> spp., <i>Cytophaga johnsonae</i>	[58–60]
Lys-, Hydroxy-Lys-FAHFA	<i>Pseudobacter saltans</i> , <i>Flavobacterium johsoniae</i> , <i>Rhizobium tropici</i>	[61–63]

Table 7. Cont.

Lipid Class	Bacterial Strains	References
Orn-FAHFA	<i>Plantomyces</i> spp., <i>Burkholderia</i> spp., <i>Rhizobium</i> spp., <i>Agrobacterium tumefaciens</i>	[1,64–66]
Gln-FAHFA, Gln-FAHFA(OH)	<i>E. coli</i>	[45]
Gly-Ser-FAHFA	<i>Flectobacillus major</i> , <i>Bacteroidetes</i> spp. including <i>P. gingivalis</i>	[67–72]
Gly-Ser-Orn-FAHFA, Gly-Ser-Orn-FAHFA(OH)	<i>Bacteroidetes</i> spp.	[71]
Gly-Ser-FAHFA-P-DG	<i>P. gingivalis</i>	[70,71]
Gly-Ser-HFA	<i>Bacteroidetes</i> spp., <i>Cryptophaga johnsonae</i>	[60,71–73]
Gly-Ser-Orn-HFA	<i>Bacteroidetes</i> spp.	[71]

1.2.3. Gram-Negative Bacteria: Modified Ceramides

Gram-negative bacteria possess several unique modified ceramides which are considered to contribute to membrane charge (Table 8).

Table 8. Gram-negative-bacterial-modified ceramides.

Lipid Class	Bacterial Strains	References
Ceramide-Phosphoethanolamine (Cer-PE)	<i>Bacteroidetes</i> spp., including <i>P. gingivalis</i> . Trace levels have been monitored in mammals.	[67,74–78]
Cer-Phosphoinositol (Cer-PI)	<i>Bacteroidetes</i> spp.	[72,75]
Cer-Phosphoglycerol (Cer-PG)	<i>Bacteroidetes</i> spp.	[67,73,76,79]
NAPE (N-acyl-phosphatidylethanolamine)	<i>E. coli</i> , <i>Bdellovibrio</i> spp. and <i>Raoultella</i> spp.	[80–83]
Acyl-PG	<i>E. coli</i> ; <i>Salmonella</i> spp., <i>Klebsiella pneumoniae</i> . Additionally, <i>C. glutamicum</i> Gram-positive bacteria and mammals.	[16,80,81,84–99]

1.2.4. Gram-Negative Bacteria: Glycosyl-Glycerophosphoalkylamines

Several complex glycolipids have been identified as regulators of cell temperature in *Thermus thermophilus* [91,92]: PLGN (Diacyl-PA-Acyl-Alkylamine-Glucosamine) and PGL (Diacyl-PA-Acyl-Alkylamine-N-Acetyl-Glucosamine).

1.2.5. Gram-Negative Bacteria: Sterols

Gram-negative bacteria utilize several unique cholesteryl acyl-glycosides as immunostimulants and hopanoids which order membrane lipids and regulate membrane permeability [97] (Table 9).

Table 9. Gram-negative bacterial sterols.

Lipid Class	Bacterial Strains	References
Cholesteryl Acyl α -Glycoside (CAG)	<i>Helicobacter pylori</i> , <i>Borrelia burgdorferi</i>	[93–96]
Cholesteryl Acyl α -Phospho-Glycoside (CPG)	<i>Helicobacter pylori</i> , <i>Borrelia burgdorferi</i>	[93–96]
Cholesteryl Phosphoethanolamine- Glycoside (CEPG)	<i>Helicobacter pylori</i>	[94]
Bacteriohopanetetrol cyclitol ethers (BHT-CE)	<i>Burkholderia</i> spp., <i>Methylobacterium organophilum</i> , <i>Chloracidobacteria</i> spp.	[98–101]

1.2.6. Gram-Negative Bacteria: Secondary Metabolites

Gram-negative bacteria produce a number of secondary metabolites that they utilize to protect against other microbes (Table 10).

Table 10. Gram-Negative Bacterial Secondary Metabolites.

Lipid Class	Bacterial Strains	References
Undecylprodigiosin metabolites	<i>Streptomyces</i> spp., <i>Serratia marcescens</i>	[102–104]
Malleilactone	<i>Burkholderia pseudomallei</i>	[105]

In summary, the wide diversity of bacterial lipids offers the potential to differentiate different bacterial species via lipidomics analyses. For example, previous studies of polar lipids in *Clostridia* spp. in four different groups of bacteria based on morphological and biochemical criteria demonstrated that three of the four groups possessed lipids that distinguished each group. All groups had high levels of PE and PG. However, Group I (*C. sporogenes* prototype) possessed PE-NAcGlu-DGs, Group II (*C. butyricum* prototype) possessed glycerol and PG acetals of ethanolamine plasmalogens, Group III (*C. novyi* prototype) possessed aminoacyl-PGs, and Group IV (*C. subterminale* prototype) had no distinguishing polar lipids [106,107]. Extending future lipidomics analyses across a broader scope than just polar lipids should further increase our ability to differentiate ongoing bacterial infections.

The objective of our study was to initiate building a bacterial lipidomics database that we could utilize to interrogate serum from cows infected with paratuberculosis and provide the groundwork required to continue building and expanding the database such that it will allow for the interrogation of other clinically relevant infections.

2. Materials and Methods

2.1. Bacterial Processing

Bacterial pellets purchased from the ATCC (Manassas, VA, USA) were sonicated (Thermo Fisher FB50) in 1 mL of methanol and 1 mL of water containing 2 nanomoles of [¹³C₃]DG 36:2 (Larodan, Monroe, MI, USA). Next 2 mL of tert-butylmethylether was added, and the samples were shaken at room temperature for 30 min (Thermo Fisher Multitube Vortexer, Waltham, MS, USA). Next, the samples were centrifuged at 4000× g for 30 min at room temperature. From the upper organic layer of these centrifuged samples, 1 mL aliquots were transferred to a deep-well microplate. The microplate samples were dried via vacuum centrifugation (Eppendorf Vacufuge Plus, Hamburg, Germany).

The Gram-positive bacterial pellets which we evaluated were *Mycobacterium avium*, ss. Paratuberculosis (ATCC 700535), *Staphylococcus aureus* (ATCC 10832), *Mycobacterium bovis* (ATCC 35737), *Mycobacterium smegmatis* (ATCC 14468), *Rhodococcus equi* (ATCC 7699), *Enterococcus faecalis* (ATCC 19433), and *Corynebacterium glutamicum* (13032). The purchased Gram-negative bacterial pellets were *Helicobacter pylori* (ATCC 43504), *Pseudomonas aeruginosa* (ATCC 10145), *Proteus mirabilis* (ATCC 12453), *Moraxella bovoculi* (ATCC BBA-1259), and *Escherichia coli* (ATCC 12435).

2.2. Lipidomics Analysis

We utilized published data and lipid databases for bacterial lipids and then incorporated them into our established lipidomics analytical platform [106,108–112] such that now we can interrogate approximately 11,000 individual lipids. As a pilot to evaluate the utility of this platform to detect active bacterial infections, we utilized the platform to examine the lipidome of a number of representative Gram-positive and Gram-negative bacteria and plasma samples from cows with paratuberculosis [112].

Specifically, to the dried samples, we added 200 µL of 2-propanol:methanol:chloroform (8:4:4), containing 5 mM ammonium chloride [108,111]. Lipids were characterized by flow infusion analysis (FIA) with electrospray ionization (ESI). FIA at 20 µL/minute was

performed utilizing high-resolution (140,000 at 200 amu) data acquisition with an orbitrap mass spectrometer (Thermo Q Exactive) [106,108–112]. The FIA included a 30 s scan in the positive ESI mode (300–1500 amu), followed by a 30 s scan in the negative ESI mode (290–1500 amu). Between sample injections, the syringe and tubing were flushed with 1 mL of methanol, followed by 1 mL of hexane: ethyl acetate: chloroform: water (3:2:1:0.1). FIA has the advantages of high sample throughput with a short analysis time for each sample and data acquisition with a constant concentration of the lipid matrix.

For MS/MS analyses, parent ions were selected with a 0.4 amu window and collision energies of 15, 30, and 50 arbitrary units. Product ions were monitored with a resolution of 240,000. Product ions with a <1.0 ppm mass error are listed in Supplementary Table S3. We utilized Lincoln Memorial University, Metabolomics Unit, Flow Infusion Lipidomics Analytical Platform (Version 1.0).

2.3. Bovine PTB Serum Samples

Serum samples (100 μ L) from our previous research [112] were used for this study and processed as described above. The cattle ($n = 10$) were 2-to-2.5-year-old angus. PTB infection was confirmed utilizing enzyme-linked immunosorbent assay (ELISA) (IDEXX MAP ELISA Ab Test kit, Westbrook, ME, USA). All testing was performed at the University of Kentucky Veterinary Diagnostic Laboratory (UKVDL), a fully accredited laboratory of the American Association of Veterinary Laboratory Diagnosticians (AAVLD).

2.4. Data Reduction

To our established in-house lipid database in Excel (Microsoft 365), we added the exact masses for a large number of individual bacterial lipids. Exact masses were obtained from online databases and the published literature. The databases we used included LipidMaps [PMID 33037133], *E. coli* Metabolome Database (ECMDB) [PMID 26481353], Yeast Metabolome Database (YMDB) [PMID 27899612], Mycobacterium tuberculosis Database (Mtb LipidDB) [PMID 21285232], Chemical Entities of Biological Interest (ChEBI) [PMID 26467479], Human Metabolome Database (HMDB) [PMID 34986597], Seaweed Metabolite Database (SWMD) [PMID 21423723], PubChem [PMID 33151290], and PubMed [PMID 33085945].

Mass spectrometric data were imported into this spreadsheet. This included individual scanned masses and their associated peak intensities. Based on the infusion solvent, the predominant ions were $[M+H]^+$ or $[M+NH_4]^+$ in positive electrospray ionization (PESI), and they were $[M-H]^-$ or $[M+Cl]^-$ in NESI [108,111]. To define which ions were optimal for different lipid families, along with defining MS/MS criteria for structural validation, we purchased a number of microbial lipid standards. This included mycolic acids (Cat. 791280 and 791282), acyl-ceramides (Cat. 860626), lysyl-PG (Cat. 840521), sulfogalactosyl-ceramides (Cat. 860571), monogalactosyl-DG (Cat. 840523), and digalactosyl-DG (Cat. 840524) from Avanti Polar Lipids (Alabaster, AL, USA) and lipid A variants (Cat. SML-2430, Cat. L6895, and L5399), acyl trehalose (Cat. 30564), trehalose dimycolates (Cat. T3034), and rhamnolipids (Cat. R95MD and R95DD) from Sigma-Aldrich (St. Louis, MO, USA) to gain practical experience. In the case of lipid classes for which analytical standards were not available, we utilized the experiences from the prior literature and our in-house experience with our infusion solvent.

For each lipid in the Excel mass list, the imported data were searched for a matching mass with <1.0 ppm mass error. For positive hits, the extracted mass and the associated peak intensity were imported into a new active spreadsheet. The specific details for each lipid class, along with the associated ionization modes and MS/MS products, are presented in Supplementary Table S3, which details all the lipid classes included in our lipidomics analytical platform, along with citations for representative publications.

3. Results

3.1. Gram-Positive Bacteria

3.1.1. *M. avium* Specific Lipids: Phthiodiolone Dimycocerosates and Diacyltrehaloses

M. avium was unique in that it was the only Gram-positive species we examined that possessed phthiodiolone dimycocerosates and diacyltrehaloses (Figure 1 and Supplementary Table S1). The phthiodiolone dimycocerosates (PDIMs) are long-chain β -diols esterified at the hydroxy groups with multimethyl-branched fatty acids (mycocerosic acids). We specifically monitored PDIM-B forms in which a position 2 of the diol is a keto group. The dominant member of this lipid family was PDIM-B C82 in the ATCC bacterial pellets and was detected in the serum of cattle with paratuberculosis but not in control cows (Figure 1 and Supplementary Table S1). In contrast, while we detected diacyltrehaloses in the *M. avium* bacterial pellet (Supplementary Table S1), these lipids were undetectable in the serum of infected cows. The diacyltrehaloses were in the DAT2 family which have a fatty acid (16:0 to 19:0) and a mycolipanic fatty acid substituent. The mycolipanic fatty acids were 3-hydroxy-2,4,6-methyl fatty acids of 24 to 28 carbons.

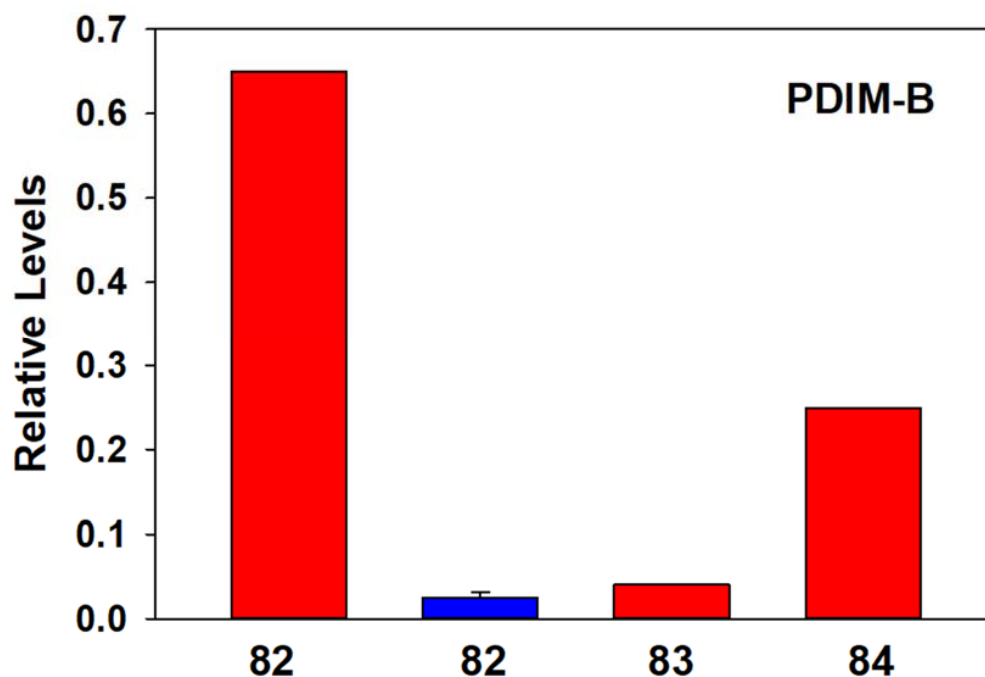


Figure 1. Relative PDIM-B levels in the bacterial pellet of *M. avium* (Red bars) and in the serum of 10 cows infected with PTB (blue bar; mean \pm SD).

3.1.2. Trehalose Mycolates

Hydroxy-trehalose monomycolates (hTMMs) were monitored in all of the examined bacteria except for *S. aureus* and *E. faecalis* (Supplementary Table S1). Each bacterial strain had a different dominant hTMM. In the case of *M. avium*, hTMM 28:1 was the dominant member of the lipid family and was also detected in the serum of PTB-positive cattle (Figure 2). While acetylTMMs were monitored in *M. avium* and a number of other Gram-positive bacteria (Supplementary Table S1), we did not detect any of this lipid family in the serum of infected cows.

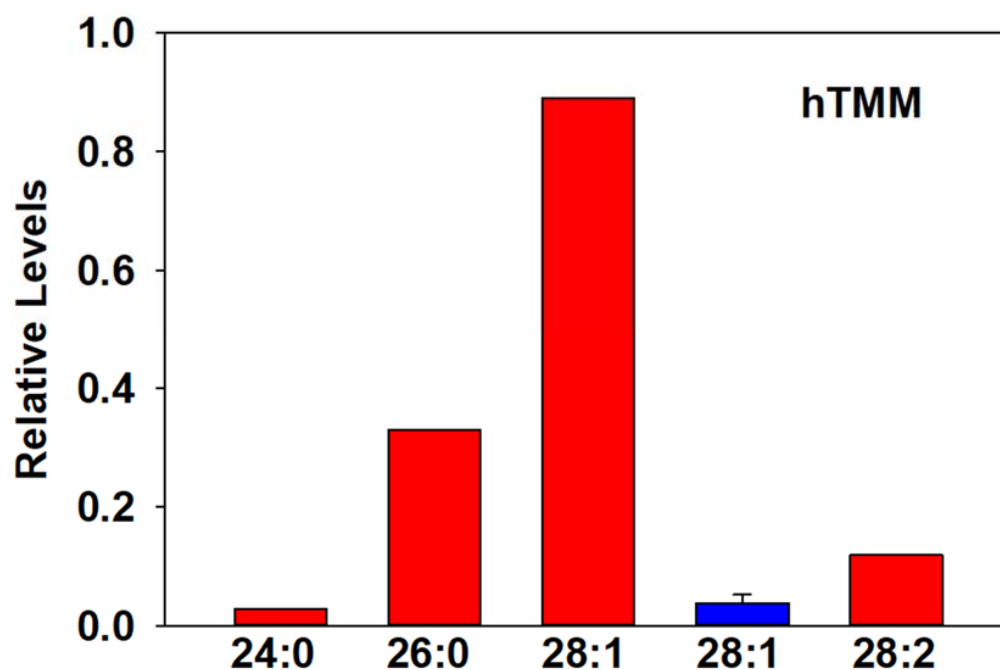


Figure 2. Relative hTMM levels in the bacterial pellet of *M. avium* (Red bars) and in the serum of 10 cows infected with PTB (blue bar; mean \pm SD).

3.1.3. Lipoteichoic Acid Precursors

Lipoteichoic acid precursors (LTAPs; dihexosyldiacylglycerol-glycerol phosphate), along with the mono-alanine and di-alanine analogs, were not detected in the *M. avium* bacterial pellet (Supplementary Table S1). LTAP 32:0 was monitored in *S. aureus*, while LTAPs and Ala-LTAPs were monitored in the bacterial pellets from *R. equi*, *E. faecalis*, and *C. glutamicum*. As with other lipids, the dominant LTAP lipid family member was different for each bacterial strain. Di-Ala-LTAPs were detected only in *R. equi* bacterial pellets.

3.1.4. Mannosyl Phosphoinositols (PIM1)

Acyl-PIM1 family members were only monitored in the *C. glutamicum* bacterial pellets (Supplementary Table S1), consistent with prior studies [16]. The acyl-PIM1 family has also been reported for a number of *Mycobacteria* [41]; however, we did not detect any acyl-PIM1 in the *Mycobacteria* we studied. This may have resulted from low levels and/or ion suppression.

3.1.5. Mycolic Acids

All of the Gram-positive bacteria that we studied were found to contain mycolic acids (Figures 3 and 4; Supplementary Table S1). A diverse array of mycolic acids was monitored in the bacterial pellets. Most mycolic acids are tethered in the outer membrane, but there are small membrane levels of free mycolic acids [31–34,113], as demonstrated in Figures 3 and 4. For the unsaturated lipids, our data do not distinguish between a double bond or a cyclopropyl substitution [113]. Both *M. bovis* and *M. smegmatis* mycolic acids were skewed to a distribution of longer-chain fatty acyl substituents (Figure 4). Interestingly, only these two bacterial strains had measurable levels of epoxy mycolic acids (Supplementary Table S1). It also needs to be noted that our analyses do not distinguish between the isobars of oxygenated lipids [113]. For example, epoxy mycolic acid 77:1 = ketomycolic acid 77:1 = methoxy mycolic acid 77:2.

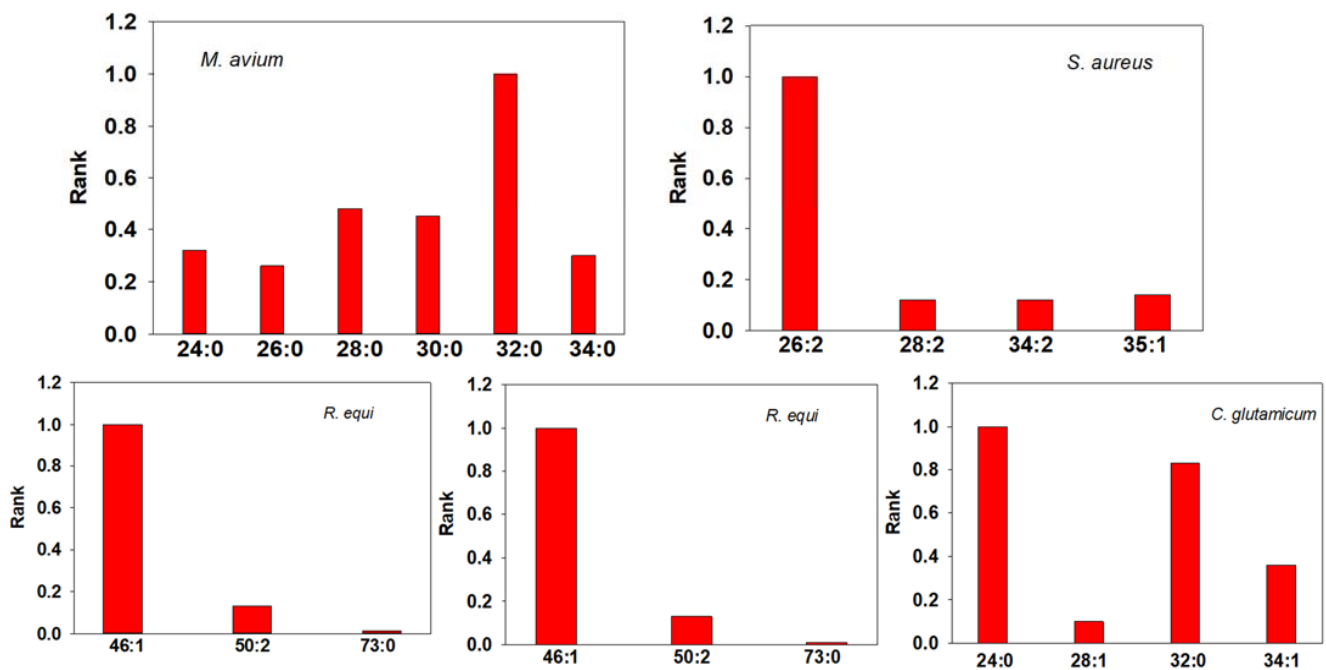


Figure 3. Bacterial mycolic acid levels presented as a rank order for *M. avium*, *S. aureus*, *R. equi*, *E. faecalis*, and *C. glutamicum*. The data are presented in Supplementary Table S1. With FIA, we cannot distinguish between double bonds and cyclopropane groups in the mycolic acids designated as unsaturated.

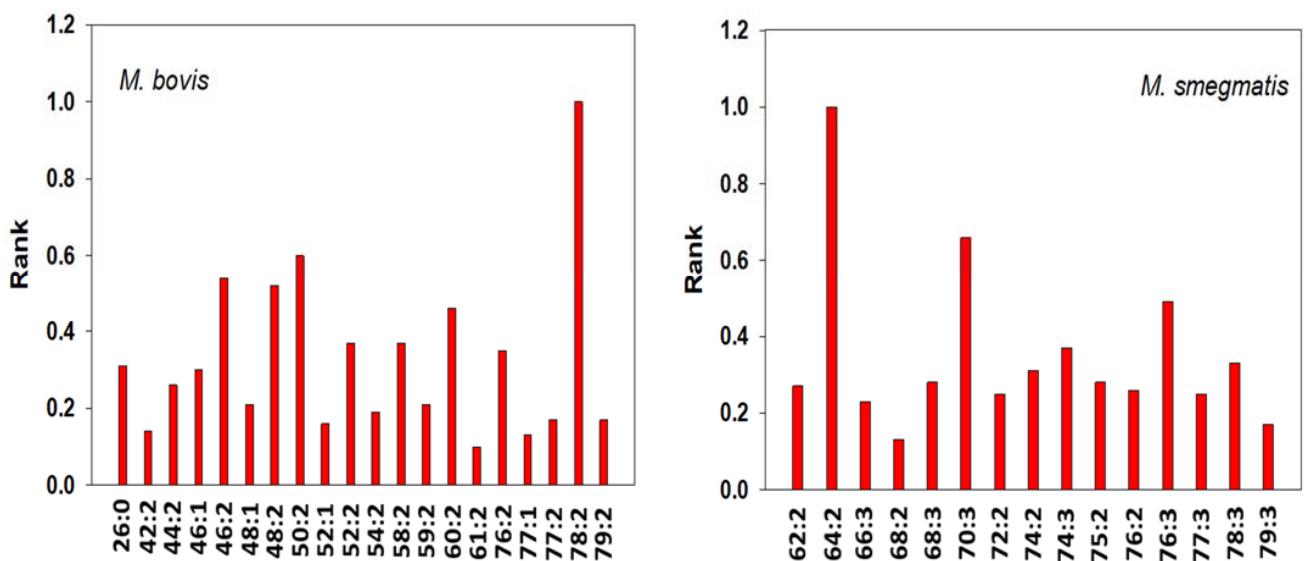


Figure 4. Bacterial mycolic acid levels presented as a rank order for *M. bovis* and *M. smegmatis*. The data are presented in Supplementary Table S1. With FIA, we cannot distinguish between double bonds and cyclopropane groups in the mycolic acids designated as unsaturated.

Dicarboxylic mycolic acids were only detected in *M. avium* and *M. bovis* (Supplementary Table S1).

The complexity of mycolic acids in bacteria was reflected in our analysis of the serum from cows infected with PTB. Four of the ten cows had levels of mycolic acid 50:2 (0.0011 ± 0.00064), five cows had dicarboxylic acid 82:1 (0.0053 ± 0.00065), two cows had dicarboxylic mycolic acid 84:1, one cow had dicarboxylic mycolic acid 82:2, and one cow had dicarboxylic mycolic acid 84:2. These lipids were not detected in the 10 control cows. This heterogeneity of detectable mycolic acids in the serum of infected cows may be

reflective of different stages of the PTB infection, which is known to progress slowly over time [114].

3.1.6. Glycopeptidolipids (GPLs)

The cell walls of a number of *Mycobacteria* contain a family of unique GPLs that consist of a hydroxy fatty acid coupled to a peptide which in turn is coupled to rhamnose [115–117]. The hydroxy fatty acid has a deoxytalose (dTal) glycation which has 0-to-2 possible acetylations. The peptide is Phe-Thr-Ala-Alaninol, and the terminal rhamnose has 0-to-3 possible O-methylations. This lipid family serves as cell-surface antigens.

We monitored an array of GPLs with the rank order of prevalence *C. glutamicum* > *M. smegmatis* > *R. equi* > *M. bovis* (Supplementary Table S1).

3.1.7. Sulfonolipids

Sulfonolipids are characterized by the replacement of serine in the sphingolipid base by the sulfonic acid caprine generating sulfobacins (monohydroxy) and sulfocristamides (di-hydroxy) [118]. These lipids are required for gliding motility and demonstrate pro-inflammatory and cytotoxic activities [118]. Both *C. glutamicum* and *M. bovis* were found to possess these highly charged sphingolipids (Supplementary Table S1).

3.1.8. Alpha-Acyl Hydroxy Fatty Acids (AAHFAs)

AAHFAs are a unique family of FAHFA lipids in which case the acylation is at a hydroxy group on carbon 2, with the acyl substitution being butyric acid [119]. The functions of these newly discovered lipids remain to be elaborated. In our analyses, we found high levels of AAHFAs in *M. avium* and moderate levels in *S. aureus* and *M. bovis* (Supplementary Table S1).

3.2. Gram-Negative Bacteria

Gram-negative bacteria lack the cell wall characteristic of Gram-positive bacteria. Lipid A is a major membrane lipid in the cell envelope, comprising an inner and outer membrane with an intermediate peptidoglycan layer. While intact lipid A molecules are large and tethered, a number of lipid A precursors are easily analyzed via conventional lipid-extraction procedures. Modified fatty acyls of hydroxy fatty acids (FAHFAs) are one example of these lipid A constituents that are absent from Gram-positive bacteria.

3.2.1. Aminoacyl FAHFAs

FAHFAs are present in mammals, but the aminoacyl forms of these lipids are not [49]. Aminoacyl FAHFAs are unique to Gram-negative bacteria. In our study, we monitored glycyl-, lysyl-, hydroxylysyl-, glutaminy-, and ornithinyl-FAHFAs in the Gram-negative bacteria we evaluated. Orn-FAHFA (Figure 5) and Gly-FAHFA were monitored in all bacteria examined, while Ala-FAHFA was absent from *H. pylori* (Supplementary Table S2).

Gly-Ser-FAHFAs are characteristic of some Gram-negative bacteria [73,77]. We monitored these unique dipeptide lipids in *P. mirabilis* and *M. bovoculi* (Supplementary Table S2). Gly-Ser-hydroxy-fatty acids were also monitored in these two bacterial strains, as well as in *H. pylori*.

Aminoacyl FAHFAs have long been conjectured to play a role in replacing glycerophospholipids in membranes, where they regulate membrane charge. Other studies have also demonstrated their roles in signal transduction. For example, ornithine lipids act at GPCRs involved in immune activation [65]. Similarly, Gly-Ser lipids act at Toll-like 2 receptors involved in immunostimulation [69,70].

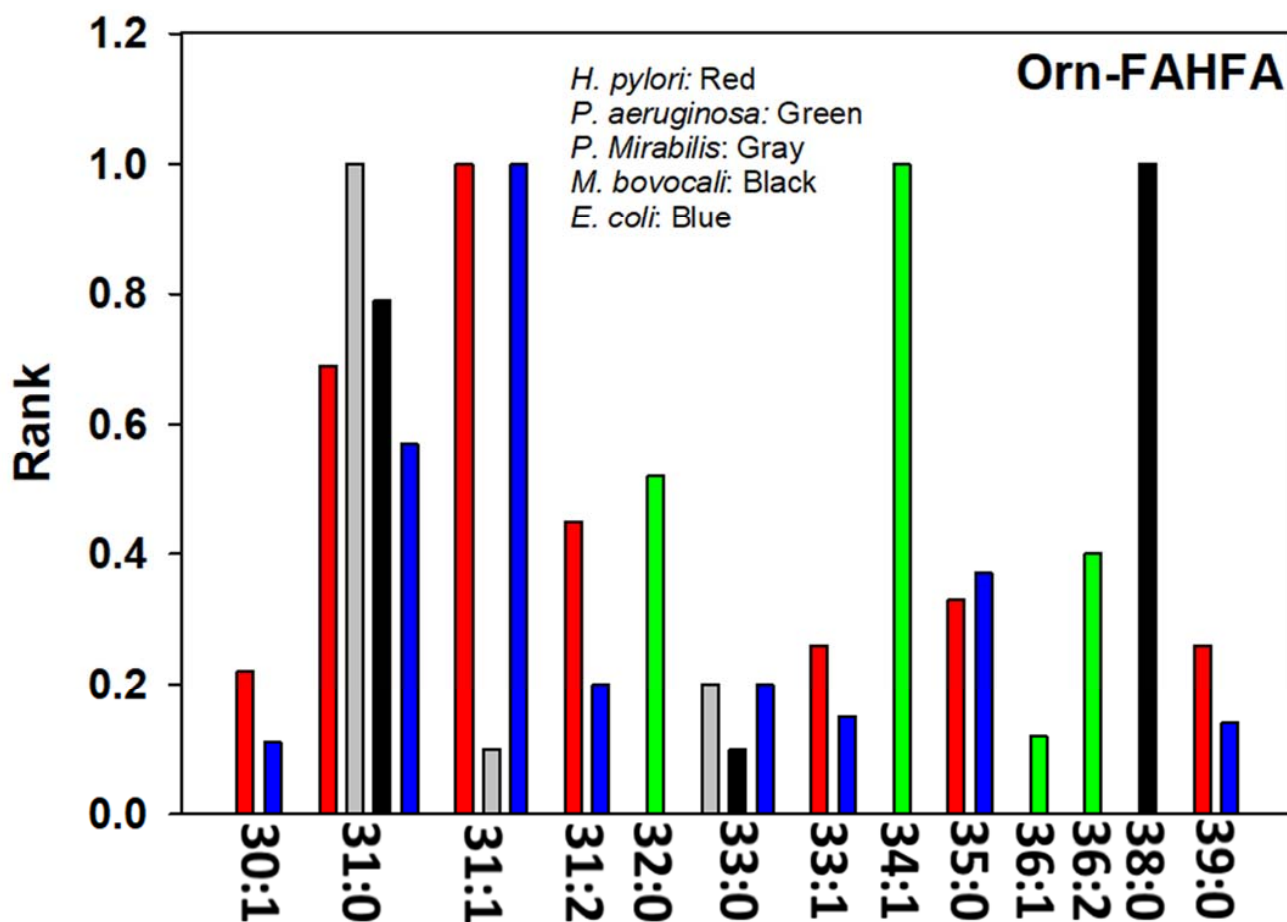


Figure 5. Bacterial ornithinyl-FAHFA levels presented as a rank order for each Gram-negative bacterial strain. The data are presented in Supplementary Table S1.

3.2.2. Modified Ceramides

The addition of a polar phosphoethanolamine or phosphoglycerol group to ceramides has been shown to be another unique feature of a number of Gram-negative bacteria [64,67,73–77,79]. We monitored a diverse array of these lipids in *H. pylori*, *P. mirabilis*, and *M. bovocali* but not in *E. coli* or *P. aeruginosa* (Supplementary Table S2).

3.2.3. Unique Sterols

Cholesteryl-acylphosphoglycosides (CPGs) have been detected in *H. pylori* [93,94] and *Borella burgdorferi* [95,96]. We confirm that *H. pylori* has these unique lipids and report for the first time that *P. mirabilis* also has these membrane lipids (Supplementary Table S2).

3.2.4. Phosphatidyltrehalose (PT)

Phosphatidyltrehaloses have been reported for *Salmonella paratyphi* and *S. typhi* [120]. We report for the first time that these immunostimulant lipids are also present in *P. mirabilis* and *E. coli* (Supplementary Table S2).

4. Discussion

Our data support previous studies demonstrating the stark contrast of the lipidomes of Gram-positive and Gram-negative bacteria. Furthermore, by utilizing a standard lipid-extraction procedure, we were able to demonstrate the presence of both PDIM-B C82, a phthiodiolone dimycocerosate, and the trehalose monomycolate hTMM 28:1 in the plasma of cows with PTB. These specific constituents of the bacterial cell envelope in *M. avium* are the dominant family members we extracted from commercial bacterial pellets. Serum

mycolic acids were also detected, but the levels were much more variable. Our data demonstrate the power and specificity of lipidomics to detect bacterial infections. Presumably, targeted assays to provide absolute lipid levels will provide even more specificity and sensitivity.

Lipid biomarkers have been utilized previously to demonstrate the presence of tuberculosis in archaeological samples [121–125] and to monitor Gram-negative bacterial infections in carotid atheroma (Gly-Ser-lipids) [73] and in oral samples from patients with periodontitis [77]. These and our current data support the idea of building a database of microbial lipids of interest to human and veterinary clinical medicine. Such a database will, in turn, yield the data required to determine which lipids might be of value to establish absolute quantitation clinical assays.

5. Study Limitations

This is the first step in building a comprehensive bacterial lipidomics database that will be expanded as we add the profiles of other bacteria to increase its applicability to bacterial research. Our FIA methodology has the strengths of covering a broader range of lipids and providing a stable and constant background, compared to hybrid chromatographic methods. However, issues with isobars are more prevalent with FIA. To reduce this risk, we utilized HRMS and only accepted lipids that were <1.0 ppm mass error. We also utilized MS² to validate the lipid identities. The MS² parameters for each lipid class are presented in Supplementary Table S3: Lincoln Memorial University, Metabolomics Unit, Flow Infusion Lipidomics Analytical Platform (Version 1.0).

Supplementary Materials: The following supporting information, in a single file, can be downloaded at <https://www.mdpi.com/article/10.3390/metabo13070809/s1>. Table S1: Rank order of lipid families in Gram-positive bacteria. Table S2: Rank order of lipid families in Gram-negative bacteria. Table S3: Lincoln Memorial University, Metabolomics Unit, Flow Infusion Lipidomics Analytical Platform (Version 1.0).

Author Contributions: Both authors were responsible for the conceptualization and conduct of the study. P.L.W. was responsible for the methodology, data reduction software, validation and formal analysis, investigation, resources, data curation, and the original draft preparation. Both authors were responsible for the manuscript review and editing. All authors have read and agreed to the published version of the manuscript.

Funding: This research was funded by Lincoln Memorial University.

Institutional Review Board Statement: Not applicable.

Informed Consent Statement: Not applicable.

Data Availability Statement: All data are in the manuscript.

Conflicts of Interest: The authors declare no conflict of interest.

References

1. Sohlenkamp, C.; Geiger, O. Bacterial membrane lipids: Diversity in structures and pathways. *FEMS Microbiol. Rev.* **2016**, *40*, 133–159. [[CrossRef](#)] [[PubMed](#)]
2. Shiraishi, T.; Yokota, S.; Fukiya, S.; Yokota, A. Structural diversity and biological significance of lipoteichoic acid in Gram-positive bacteria: Focusing on beneficial probiotic lactic acid bacteria. *Biosci. Microbiota Food Health* **2016**, *35*, 147–161. [[CrossRef](#)] [[PubMed](#)]
3. Adams, H.M.; Joyce, L.R.; Guan, Z.; Akins, R.L.; Palmer, K.L. *Streptococcus mitis* and *S. oralis* Lack a Requirement for CdsA, the Enzyme Required for Synthesis of Major Membrane Phospholipids in Bacteria. *Antimicrob. Agents Chemother.* **2017**, *61*, e02552-16. [[CrossRef](#)] [[PubMed](#)]
4. Wei, Y.; Joyce, L.R.; Wall, A.M.; Guan, Z.; Palmer, K.L. *Streptococcus pneumoniae*, *S. mitis*, and *S. oralis* Produce a Phosphatidylglycerol-Dependent, ItaS-Independent Glycerophosphate-Linked Glycolipid. *mSphere* **2021**, *6*, e01099-20. [[CrossRef](#)] [[PubMed](#)]
5. Guan, Z.; Garrett, T.A.; Goldfine, H. Lipidomic Analysis of *Clostridium cadaveris* and *Clostridium fallax*. *Lipids* **2019**, *54*, 423–431. [[CrossRef](#)] [[PubMed](#)]
6. Sallans, L.; Giner, J.L.; Kiemle, D.J.; Custer, J.E.; Kaneshiro, E.S. Structural identities of four glycosylated lipids in the oral bacterium *Streptococcus mutans* UA159. *Biochim. Biophys. Acta* **2013**, *1831*, 1239–1249. [[CrossRef](#)] [[PubMed](#)]

7. Guan, Z.; Chen, L.; Gerritsen, J.; Smidt, H.; Goldfine, H. The cellular lipids of *Romboutsia*. *Biochim. Biophys. Acta* **2016**, *1861 Pt A*, 1076–1082. [[CrossRef](#)] [[PubMed](#)]
8. Lopes, C.; Barbosa, J.; Maciel, E.; da Costa, E.; Alves, E.; Domingues, P.; Mendes, S.; Domingues, M.R.M. Lipidomic signature of *Bacillus licheniformis* I89 during the different growth phases unravelled by high-resolution liquid chromatography-mass spectrometry. *Arch. Biochem. Biophys.* **2019**, *663*, 83–94. [[CrossRef](#)] [[PubMed](#)]
9. Guan, Z.; Goldfine, H. Lipid diversity in clostridia. *Biochim. Biophys. Acta Mol. Cell Biol. Lipids* **2021**, *1866*, 158966. [[CrossRef](#)] [[PubMed](#)]
10. Harrison, N.A.; Gardner, C.L.; da Silva, D.R.; Gonzalez, C.F.; Lorca, G.L. Identification of Biomarkers for Systemic Distribution of Nanovesicles from *Lactobacillus johnsonii* N6.2. *Front. Immunol.* **2021**, *12*, 723433. [[CrossRef](#)] [[PubMed](#)]
11. Webb, A.J.; Karatsa-Dodgson, M.; Gründling, A. Two-enzyme systems for glycolipid and polyglycerolphosphate lipoteichoic acid synthesis in *Listeria monocytogenes*. *Mol. Microbiol.* **2009**, *74*, 299–314. [[CrossRef](#)] [[PubMed](#)]
12. Luo, Y. Alanylated lipoteichoic acid primer in *Bacillus subtilis*. *F1000Research* **2016**, *5*, 155. [[CrossRef](#)] [[PubMed](#)]
13. Atila, M.; Luo, Y. Profiling and tandem mass spectrometry analysis of aminoacylated phospholipids in *Bacillus subtilis*. *F1000Research* **2016**, *5*, 121. [[CrossRef](#)] [[PubMed](#)]
14. Percy, M.G.; Karinou, E.; Webb, A.J.; Gründling, A. Identification of a Lipoteichoic Acid Glycosyltransferase Enzyme Reveals that GW-Domain-Containing Proteins Can Be Retained in the Cell Wall of *Listeria monocytogenes* in the Absence of Lipoteichoic Acid or Its Modifications. *J. Bacteriol.* **2016**, *198*, 2029–2042. [[CrossRef](#)] [[PubMed](#)]
15. Smith, A.M.; Harrison, J.S.; Grube, C.D.; Sheppe, A.E.; Sahara, N.; Ishii, R.; Nureki, O.; Roy, H. tRNA-dependent alanylation of diacylglycerol and phosphatidylglycerol in *Corynebacterium glutamicum*. *Mol. Microbiol.* **2015**, *98*, 681–693. [[CrossRef](#)] [[PubMed](#)]
16. Klatt, S.; Brammananth, R.; O’Callaghan, S.; Kouremenos, K.A.; Tull, D.; Crellin, P.K.; Coppel, R.L.; McConville, M.J. Identification of novel lipid modifications and intermembrane dynamics in *Corynebacterium glutamicum* using high-resolution mass spectrometry. *J. Lipid Res.* **2018**, *59*, 1190–1204, Outstanding publication. A must read. [[CrossRef](#)] [[PubMed](#)]
17. Tatituri, R.V.V.; Hsu, F.F. Characterization of the Uncommon Lipid Families in *Corynebacterium glutamicum* by Mass Spectrometry. *Methods Mol. Biol.* **2021**, *306*, 227–238. [[PubMed](#)]
18. Wang, H.J.; Tatituri, R.V.V.; Goldner, N.K.; Dantas, G.; Hsu, F.F. Unveiling the biodiversity of lipid species in *Corynebacteria*-characterization of the uncommon lipid families in *C. glutamicum* and pathogen *C. striatum* by mass spectrometry. *Biochimie* **2020**, *178*, 158–169, Outstanding publication. A must read. [[CrossRef](#)] [[PubMed](#)]
19. Luo, Y.; Javed, M.A.; Deneer, H. Comparative study on nutrient depletion-induced lipidome adaptations in *Staphylococcus haemolyticus* and *Staphylococcus epidermidis*. *Sci. Rep.* **2018**, *8*, 2356. [[CrossRef](#)] [[PubMed](#)]
20. Joyce, L.R.; Manzer, H.S.; da Mendonça, J.; Villarreal, R.; Nagao, P.E.; Doran, K.S.; Palmer, K.L.; Guan, Z. Identification of a novel cationic glycolipid in *Streptococcus agalactiae* that contributes to brain entry and meningitis. *PLoS Biol.* **2022**, *20*, e3001555. [[CrossRef](#)] [[PubMed](#)]
21. Johnston, N.C.; Aygun-Sunar, S.; Guan, Z.; Ribeiro, A.A.; Daldal, F.; Raetz, C.R.; Goldfine, H. A phosphoethanolamine-modified glycosyl diradylglycerol in the polar lipids of *Clostridium tetani*. *J. Lipid Res.* **2010**, *51*, 1953–1961. [[CrossRef](#)] [[PubMed](#)]
22. Guan, Z.; Johnston, N.C.; Aygun-Sunar, S.; Daldal, F.; Raetz, C.R.; Goldfine, H. Structural characterization of the polar lipids of *Clostridium novyi* NT. Further evidence for a novel anaerobic biosynthetic pathway to plasmalogens. *Biochim. Biophys. Acta* **2011**, *1811*, 186–193. [[CrossRef](#)] [[PubMed](#)]
23. Slavetinsky, C.; Kuhn, S.; Peschel, A. Bacterial aminoacyl phospholipids-Biosynthesis and role in basic cellular processes and pathogenicity. *Biochim. Biophys. Acta Mol. Cell Biol. Lipids* **2017**, *1862*, 1310–1318. [[CrossRef](#)] [[PubMed](#)]
24. Roy, H. Tuning the properties of the bacterial membrane with aminoacylated phosphatidylglycerol. *IUBMB Life* **2009**, *61*, 940–953. [[CrossRef](#)] [[PubMed](#)]
25. Atila, M.; Katselis, G.; Chumala, P.; Luo, Y. Characterization of N-Succinylation of L-Lysylphosphatidylglycerol in *Bacillus subtilis* Using Tandem Mass Spectrometry. *J. Am. Soc. Mass Spectrom.* **2016**, *27*, 1606–1613. [[CrossRef](#)] [[PubMed](#)]
26. Khuller, G.K.; Subrahmanyam, D. On the ornithinyl ester of phosphatidylglycerol of *Mycobacterium 607*. *J. Bacteriol.* **1970**, *101*, 654–656. [[CrossRef](#)] [[PubMed](#)]
27. Kato, M.; Asamizu, S.; Onaka, H. Intimate relationships among actinomycetes and mycolic acid-containing bacteria. *Sci. Rep.* **2022**, *12*, 7222. [[CrossRef](#)] [[PubMed](#)]
28. Rahlwes, K.C.; Sparks, I.L.; Morita, Y.S. Cell Walls and Membranes of Actinobacteria. *Subcell Biochem.* **2019**, *92*, 417–469. [[PubMed](#)]
29. Blevins, M.S.; Klein, D.R.; Brodbelt, J.S. Localization of Cyclopropane Modifications in Bacterial Lipids via 213 nm Ultraviolet Photodissociation Mass Spectrometry. *Anal. Chem.* **2019**, *91*, 6820–6828. [[CrossRef](#)] [[PubMed](#)]
30. Madacki, J.; Laval, F.; Grzegorzewicz, A.; Lemassu, A.; Záhorská, M.; Arand, M.; McNeil, M.; Daffé, M.; Jackson, M.; Lanéelle, M.A.; et al. Impact of the epoxide hydrolase EphD on the metabolism of mycolic acids in mycobacteria. *J. Biol. Chem.* **2018**, *293*, 5172–5184. [[CrossRef](#)] [[PubMed](#)]
31. Hsu, F.F.; Soehl, K.; Turk, J.; Haas, A. Characterization of mycolic acids from the pathogen *Rhodococcus equi* by tandem mass spectrometry with electrospray ionization. *Anal. Biochem.* **2011**, *409*, 112–122. [[CrossRef](#)] [[PubMed](#)]
32. Hsu, F.F.; Wohlmann, J.; Turk, J.; Haas, A. Structural definition of trehalose 6-monomycolates and trehalose 6,6'-dimycolates from the pathogen *Rhodococcus equi* by multiple-stage linear ion-trap mass spectrometry with electrospray ionization. *J. Am. Soc. Mass Spectrom.* **2011**, *22*, 2160–2170. [[CrossRef](#)] [[PubMed](#)]

33. Gein, S.V.; Kochina, O.A.; Kuyukina, M.S.; Klimenko, D.P.; Ivshina, I.B. Effects of Monoacyltrehalose Fraction of Rhodococcus Biosurfactant on the Innate and Adaptive Immunity Parameters In Vivo. *Bull. Exp. Biol. Med.* **2020**, *169*, 474–477. [[CrossRef](#)] [[PubMed](#)]
34. Purdy, G.E.; Hsu, F.F. Complete Characterization of Polyacyltrehaloses from *Mycobacterium tuberculosis* H37Rv Biofilm Cultures by Multiple-Stage Linear Ion-Trap Mass Spectrometry Reveals a New Tetraacyltrehalose Family. *Biochemistry* **2021**, *60*, 381–397. [[CrossRef](#)] [[PubMed](#)]
35. Gilleron, M.; Stenger, S.; Mazorra, Z.; Wittke, F.; Mariotti, S.; Böhmer, G.; Prandi, J.; Mori, L.; Puzo, G.; De Libero, G. Diacylated sulfoglycolipids are novel mycobacterial antigens stimulating CD1-restricted T cells during infection with *Mycobacterium tuberculosis*. *J. Exp. Med.* **2004**, *199*, 649–659. [[CrossRef](#)] [[PubMed](#)]
36. Layre, E.; Cala-De Paepe, D.; Larrouy-Maumus, G.; Vaubourgeix, J.; Mundayoor, S.; Lindner, B.; Puzo, G.; Gilleron, M. Deciphering sulfoglycolipids of *Mycobacterium tuberculosis*. *J. Lipid Res.* **2011**, *52*, 1098–1110. [[CrossRef](#)] [[PubMed](#)]
37. Seeliger, J.C.; Holsclaw, C.M.; Schelle, M.W.; Botyanszki, Z.; Gilmore, S.A.; Tully, S.E.; Niederweis, M.; Cravatt, B.F.; Leary, J.A.; Bertozzi, C.R. Elucidation and chemical modulation of sulfolipid-1 biosynthesis in *Mycobacterium tuberculosis*. *J. Biol. Chem.* **2012**, *287*, 7990–8000. [[CrossRef](#)] [[PubMed](#)]
38. Rens, C.; Chao, J.D.; Sexton, D.L.; Tocheva, E.I.; Av-Gay, Y. Roles for phthiocerol dimycocerosate lipids in *Mycobacterium tuberculosis* pathogenesis. *Microbiology* **2021**, *167*, 001042. [[CrossRef](#)] [[PubMed](#)]
39. Flentie, K.N.; Stallings, C.L.; Turk, J.; Minnaard, A.J.; Hsu, F.F. Characterization of phthiocerol and phthiodiolone dimycocerosate esters of *M. tuberculosis* by multiple-stage linear ion-trap MS. *J. Lipid Res.* **2016**, *57*, 142–155. [[CrossRef](#)] [[PubMed](#)]
40. Hayashi, J.M.; Luo, C.Y.; Mayfield, J.A.; Hsu, T.; Fukuda, T.; Walfield, A.L.; Giffen, S.R.; Leszyk, J.D.; Baer, C.E.; Bennion, O.T.; et al. Spatially distinct and metabolically active membrane domain in mycobacteria. *Proc. Natl. Acad. Sci. USA* **2016**, *113*, 5400–5405. [[CrossRef](#)] [[PubMed](#)]
41. Toyonaga, K.; Torigoe, S.; Motomura, Y.; Kamichi, T.; Hayashi, J.M.; Morita, Y.S.; Noguchi, N.; Chuma, Y.; Kiyohara, H.; Matsuo, K.; et al. C-Type Lectin Receptor DCAR Recognizes Mycobacterial Phosphatidyl-Inositol Mannosides to Promote a Th1 Response during Infection. *Immunity* **2016**, *45*, 1245–1257. [[CrossRef](#)] [[PubMed](#)]
42. Zhang, J.; Liang, Q.; Xu, Z.; Cui, M.; Zhang, Q.; Abreu, S.; David, M.; Lejeune, C.; Chaminade, P.; Virolle, M.J.; et al. The Inhibition of Antibiotic Production in *Streptomyces coelicolor* Over-Expressing the TetR Regulator SCO3201 IS Correlated with Changes in the Lipidome of the Strain. *Front. Microbiol.* **2020**, *11*, 1399. [[CrossRef](#)] [[PubMed](#)]
43. Bieberich, E.; Kawaguchi, T.; Yu, R.K. N-acylated serinol is a novel ceramide mimic inducing apoptosis in neuroblastoma cells. *J. Biol. Chem.* **2000**, *275*, 177–181. [[CrossRef](#)] [[PubMed](#)]
44. Wen, S.; Ye, L.; Liu, D.; Yang, B.; Man, M.Q. Topical N-palmitoyl serinol, a commensal bacterial metabolite, prevents the development of epidermal permeability barrier dysfunction in a murine model of atopic dermatitis-like skin. *Can. J. Vet. Res.* **2021**, *85*, 201–204. [[PubMed](#)]
45. Cohen, L.J.; Esterhazy, D.; Kim, S.H.; Lemetre, C.; Aguilar, R.R.; Gordon, E.A.; Pickard, A.J.; Cross, J.R.; Emiliano, A.B.; Han, S.M.; et al. Commensal bacteria make GPCR ligands that mimic human signalling molecules. *Nature* **2017**, *549*, 48–53. [[CrossRef](#)] [[PubMed](#)]
46. Buré, C.; Le Sénéchal, C.; Macias, L.; Tokarski, C.; Vilain, S.; Brodbelt, J.S. Characterization of Isomers of Lipid A from *Pseudomonas aeruginosa* PAO1 by Liquid Chromatography with Tandem Mass Spectrometry with Higher-Energy Collisional Dissociation and Ultraviolet Photodissociation. *Anal. Chem.* **2021**, *93*, 4255–4262. [[CrossRef](#)] [[PubMed](#)]
47. Froning, M.; Helmer, P.O.; Hayen, H. Identification and structural characterization of lipid A from *Escherichia coli*, *Pseudomonas putida* and *Pseudomonas taiwanensis* using liquid chromatography coupled to high-resolution tandem mass spectrometry. *Rapid Commun. Mass Spectrom.* **2020**, *34*, e8897. [[CrossRef](#)] [[PubMed](#)]
48. Larrouy-Maumus, G. Shotgun Bacterial Lipid A Analysis Using Routine MALDI-TOF Mass Spectrometry. *Methods Mol. Biol.* **2021**, *2306*, 275–283. [[PubMed](#)]
49. Wood, P.L. Fatty Acyl Esters of Hydroxy Fatty Acid (FAHFA) Lipid Families. *Metabolites* **2020**, *10*, 512. [[CrossRef](#)] [[PubMed](#)]
50. Behrens, B.; Engelen, J.; Tiso, T.; Blank, L.M.; Hayen, H. Characterization of rhamnolipids by liquid chromatography/mass spectrometry after solid-phase extraction. *Anal. Bioanal. Chem.* **2016**, *408*, 2505–2514. [[CrossRef](#)] [[PubMed](#)]
51. Zhao, F.; Shi, R.; Ma, F.; Han, S.; Zhang, Y. Oxygen effects on rhamnolipids production by *Pseudomonas aeruginosa*. *Microb. Cell Factories* **2018**, *17*, 39. [[CrossRef](#)] [[PubMed](#)]
52. El-Housseiny, G.S.; Aboshanab, K.M.; Aboulwafa, M.M.; Hassouna, N.A. Structural and Physicochemical Characterization of Rhamnolipids produced by *Pseudomonas aeruginosa* P6. *AMB Express* **2020**, *10*, 201. [[CrossRef](#)] [[PubMed](#)]
53. Hošková, M.; Ježdík, R.; Schreiberová, O.; Chudoba, J.; Šir, M.; Čejková, A.; Masák, J.; Jirků, V.; Řezanka, T. Structural and physicochemical characterization of rhamnolipids produced by *Acinetobacter calcoaceticus*, *Enterobacter asburiae* and *Pseudomonas aeruginosa* in single strain and mixed cultures. *J. Biotechnol.* **2015**, *193*, 45–51. [[CrossRef](#)] [[PubMed](#)]
54. Lybbert, A.C.; Williams, J.L.; Raghuvanshi, R.; Jones, A.D.; Quinn, R.A. Mining Public Mass Spectrometry Data to Characterize the Diversity and Ubiquity of *P. aeruginosa* Specialized Metabolites. *Metabolites* **2020**, *10*, 445. [[CrossRef](#)] [[PubMed](#)]
55. Kawakami, N.; Fujisaki, S. Undecaprenyl phosphate metabolism in Gram-negative and Gram-positive bacteria. *Biosci. Biotechnol. Biochem.* **2018**, *82*, 940–946. [[CrossRef](#)] [[PubMed](#)]

56. Wang, X.; Ribeiro, A.A.; Guan, Z.; Raetz, C.R. Identification of undecaprenyl phosphate-beta-D-galactosamine in *Francisella novicida* and its function in lipid A modification. *Biochemistry* **2009**, *48*, 1162–1172. [[CrossRef](#)] [[PubMed](#)]
57. Collins, M.D.; Goodfellow, M.; Minnikin, D.E.; Alderson, G. Menaquinone composition of mycolic acid-containing actinomycetes and some sporoactinomycetes. *J. Appl. Bacteriol.* **1985**, *58*, 77–86. [[CrossRef](#)] [[PubMed](#)]
58. Lynch, A.; Tammireddy, S.R.; Doherty, M.K.; Whitfield, P.D.; Clarke, D.J. The Glycine Lipids of *Bacteroides thetaiotaomicron* Are Important for Fitness during Growth In Vivo and In Vitro. *Appl. Environ. Microbiol.* **2019**, *85*, e02157-18. [[CrossRef](#)] [[PubMed](#)]
59. Lynch, A.; Crowley, E.; Casey, E.; Cano, R.; Shanahan, R.; McGlacken, G.; Marchesi, J.R.; Clarke, D.J. The Bacteroidales produce an N-acylated derivative of glycine with both cholesterol-solubilising and hemolytic activity. *Sci. Rep.* **2017**, *7*, 13270. [[CrossRef](#)] [[PubMed](#)]
60. Kawazoe, R.; Okuyama, H.; Reichardt, W.; Sasaki, S. Phospholipids and a novel glycine-containing lipoamino acid in *Cytophaga johnsonae* Stanier strain C21. *J. Bacteriol.* **1991**, *173*, 5470–5475. [[CrossRef](#)] [[PubMed](#)]
61. Moore, E.K.; Hopmans, E.C.; Rijpstra, W.I.; Sánchez-Andrea, I.; Villanueva, L.; Wienk, H.; Schoutsen, F.; Stams, A.J.; Sinninghe Damsté, J.S. Lysine and novel hydroxylysine lipids in soil bacteria: Amino acid membrane lipid response to temperature and pH in *Pseudopedobacter saltans*. *Front. Microbiol.* **2015**, *6*, 637. [[CrossRef](#)] [[PubMed](#)]
62. Geiger, O.; González-Silva, N.; López-Lara, I.M.; Sohlenkamp, C. Amino acid-containing membrane lipids in bacteria. *Prog. Lipid Res.* **2010**, *49*, 46–60. [[CrossRef](#)] [[PubMed](#)]
63. Vences-Guzmán, M.Á.; Guan, Z.; Ormeño-Orrillo, E.; González-Silva, N.; López-Lara, I.M.; Martínez-Romero, E.; Geiger, O.; Sohlenkamp, C. Hydroxylated ornithine lipids increase stress tolerance in *Rhizobium tropici* CIAT899. *Mol. Microbiol.* **2011**, *79*, 1496–1514. [[CrossRef](#)] [[PubMed](#)]
64. Vences-Guzmán, M.Á.; Guan, Z.; Bermúdez-Barrientos, J.R.; Geiger, O.; Sohlenkamp, C. Agrobacteria lacking ornithine lipids induce more rapid tumour formation. *Environ. Microbiol.* **2013**, *15*, 895–906. [[CrossRef](#)] [[PubMed](#)]
65. Córdoba-Castro, L.A.; Salgado-Morales, R.; Torres, M.; Martínez-Aguilar, L.; Lozano, L.; Vences-Guzmán, M.Á.; Guan, Z.; Dantán-González, E.; Serrano, M.; Sohlenkamp, C. Ornithine Lipids in *Burkholderia* spp. Pathogenicity. *Front. Mol. Biosci.* **2021**, *7*, 610932. [[CrossRef](#)] [[PubMed](#)]
66. González-Silva, N.; López-Lara, I.M.; Reyes-Lamothe, R.; Taylor, A.M.; Sumpton, D.; Thomas-Oates, J.; Geiger, O. The dioxygenase-encoding *olsD* gene from *Burkholderia cenocepacia* causes the hydroxylation of the amide-linked fatty acyl moiety of ornithine-containing membrane lipids. *Biochemistry* **2011**, *50*, 6396–6408. [[CrossRef](#)] [[PubMed](#)]
67. Batrakov, S.G.; Mosezhnyi, A.E.; Ruzhitsky, A.O.; Sheichenko, V.I.; Nikitin, D.I. The polar-lipid composition of the sphingolipid-producing bacterium *Flectobacillus major*. *Biochim. Biophys. Acta* **2000**, *1484*, 225–240. [[CrossRef](#)] [[PubMed](#)]
68. Nemati, R.; Dietz, C.; Anstadt, E.; Clark, R.; Smith, M.; Nichols, F.; Yao, X. Simultaneous Determination of Absolute Configuration and Quantity of Lipopeptides Using Chiral Liquid Chromatography/Mass Spectrometry and Diastereomeric Internal Standards. *Anal. Chem.* **2017**, *89*, 3583–3589. [[CrossRef](#)] [[PubMed](#)]
69. Clark, R.B.; Cervantes, J.L.; Maciejewski, M.W.; Farrokhi, V.; Nemati, R.; Yao, X.; Anstadt, E.; Fujiwara, M.; Wright, K.T.; Riddle, C.; et al. Serine lipids of *Porphyromonas gingivalis* are human and mouse Toll-like receptor 2 ligands. *Infect. Immun.* **2013**, *81*, 3479–3489. [[CrossRef](#)] [[PubMed](#)]
70. Nichols, F.C.; Clark, R.B.; Maciejewski, M.W.; Provatias, A.A.; Balsbaugh, J.L.; Dewhirst, F.E.; Smith, M.B.; Rahmlow, A. A novel phosphoglycerol serine-glycine lipodipeptide of *Porphyromonas gingivalis* is a TLR2 ligand. *J. Lipid Res.* **2020**, *61*, 1645–1657. [[CrossRef](#)] [[PubMed](#)]
71. Bill, M.K.; Brinkmann, S.; Oberpaul, M.; Patras, M.A.; Leis, B.; Marner, M.; Maitre, M.P.; Hammann, P.E.; Vilcinskis, A.; Schuler, S.M.M.; et al. Novel Glycerophospholipid, Lip- and N-acyl Amino Acids from Bacteroidetes: Isolation, Structure Elucidation and Bioactivity. *Molecules* **2021**, *26*, 5195. [[CrossRef](#)] [[PubMed](#)]
72. Sartorio, M.G.; Valguarnera, E.; Hsu, F.F.; Feldman, M.F. Lipidomics Analysis of Outer Membrane Vesicles and Elucidation of the Inositol Phosphoceramide Biosynthetic Pathway in *Bacteroides thetaiotaomicron*. *Microbiol. Spectr.* **2022**, *10*, e0063421. [[CrossRef](#)] [[PubMed](#)]
73. Nemati, R.; Dietz, C.; Anstadt, E.J.; Cervantes, J.; Liu, Y.; Dewhirst, F.E.; Clark, R.B.; Finegold, S.; Gallagher, J.J.; Smith, M.B.; et al. Deposition and hydrolysis of serine dipeptide lipids of Bacteroidetes bacteria in human arteries: Relationship to atherosclerosis. *J. Lipid Res.* **2017**, *58*, 1999–2007. [[CrossRef](#)] [[PubMed](#)]
74. Panevska, A.; Skočaj, M.; Križaj, I.; Maček, P.; Sepčić, K. Ceramide phosphoethanolamine, an enigmatic cellular membrane sphingolipid. *Biochim. Biophys. Acta Biomembr.* **2019**, *1861*, 1284–1292. [[CrossRef](#)] [[PubMed](#)]
75. Brown, E.M.; Ke, X.; Hitchcock, D.; Jeanfavre, S.; Avila-Pacheco, J.; Nakata, T.; Arthur, T.D.; Fornelos, N.; Heim, C.; Franzosa, E.A.; et al. Bacteroides-Derived Sphingolipids Are Critical for Maintaining Intestinal Homeostasis and Symbiosis. *Cell Host Microbe* **2019**, *25*, 668–680.e7. [[CrossRef](#)] [[PubMed](#)]
76. Nichols, F.C.; Riep, B.; Mun, J.; Morton, M.D.; Bojarski, M.T.; Dewhirst, F.E.; Smith, M.B. Structures and biological activity of phosphorylated dihydroceramides of *Porphyromonas gingivalis*. *J. Lipid Res.* **2004**, *45*, 2317–2330. [[CrossRef](#)] [[PubMed](#)]
77. Nichols, F.C.; Bhuse, K.; Clark, R.B.; Provatias, A.A.; Carrington, E.; Wang, Y.H.; Zhu, Q.; Davey, M.E.; Dewhirst, F.E. Serine/Glycine Lipid Recovery in Lipid Extracts from Healthy and Diseased Dental Samples: Relationship to Chronic Periodontitis. *Front. Oral Health* **2021**, *2*, 698481. [[CrossRef](#)] [[PubMed](#)]

78. Bickert, A.; Ginkel, C.; Kol, M.; vom Dorp, K.; Jastrow, H.; Degen, J.; Jacobs, R.L.; Vance, D.E.; Winterhager, E.; Jiang, X.C.; et al. Functional characterization of enzymes catalyzing ceramide phosphoethanolamine biosynthesis in mice. *J. Lipid Res.* **2015**, *56*, 821–835. [[CrossRef](#)] [[PubMed](#)]
79. Nichols, F.C.; Yao, X.; Bajrami, B.; Downes, J.; Finegold, S.M.; Knee, E.; Gallagher, J.J.; Housley, W.J.; Clark, R.B. Phosphorylated dihydroceramides from common human bacteria are recovered in human tissues. *PLoS ONE* **2011**, *6*, e16771. [[CrossRef](#)] [[PubMed](#)]
80. Mileykovskaya, E.; Ryan, A.C.; Mo, X.; Lin, C.C.; Khalaf, K.I.; Dowhan, W.; Garrett, T.A. Phosphatidic acid and N-acylphosphatidylethanolamine form membrane domains in *Escherichia coli* mutant lacking cardiolipin and phosphatidylglycerol. *J. Biol. Chem.* **2009**, *284*, 2990–3000. [[CrossRef](#)] [[PubMed](#)]
81. Hines, K.M.; Xu, L. Lipidomic consequences of phospholipid synthesis defects in *Escherichia coli* revealed by HILIC-ion mobility-mass spectrometry. *Chem. Phys. Lipids* **2019**, *219*, 15–22. [[CrossRef](#)] [[PubMed](#)]
82. Palyzová, A.; Marešová, H.; Novák, J.; Zahradník, J.; Řezanka, T. Effect of the anti-inflammatory drug diclofenac on lipid composition of bacterial strain *Raoultella* sp. KDF8. *Folia Microbiol.* **2020**, *65*, 763–773. [[CrossRef](#)] [[PubMed](#)]
83. Nguyen, N.A.; Sallans, L.; Kaneshiro, E.S. The major glycerophospholipids of the predatory and parasitic bacterium *Bdellovibrio bacteriovorus* HID5. *Lipids* **2008**, *43*, 1053–1063. [[CrossRef](#)] [[PubMed](#)]
84. Kobayashi, T.; Nishijima, M.; Tamori, Y.; Nojima, S.; Seyama, Y.; Yamakawa, T. Acyl phosphatidylglycerol of *Escherichia coli*. *Biochim. Biophys. Acta* **1980**, *620*, 356–363. [[PubMed](#)]
85. Nishijima, M.; Sa-Eki, T.; Tamori, Y.; Doi, O.; Nojima, S. Synthesis of acyl phosphatidylglycerol from phosphatidylglycerol in *Escherichia coli* K-12. Evidence for the participation of detergent-resistant phospholipase A and heat-labile membrane-bound factor(s). *Biochim. Biophys. Acta* **1978**, *528*, 107–118. [[PubMed](#)]
86. Appala, K.; Bimpeh, K.; Freeman, C.; Hines, K.M. Recent applications of mass spectrometry in bacterial lipidomics. *Anal. Bioanal. Chem.* **2020**, *412*, 5935–5943. [[CrossRef](#)] [[PubMed](#)]
87. Hsu, F.F.; Turk, J.; Shi, Y.; Groisman, E.A. Characterization of acylphosphatidylglycerols from *Salmonella typhimurium* by tandem mass spectrometry with electrospray ionization. *J. Am. Soc. Mass Spectrom.* **2004**, *15*, 1–11. [[PubMed](#)]
88. Dalebroux, Z.D.; Matamouros, S.; Whittington, D.; Bishop, R.E.; Miller, S.I. PhoPQ regulates acidic glycerophospholipid content of the *Salmonella typhimurium* outer membrane. *Proc. Natl. Acad. Sci. USA* **2014**, *111*, 1963–1968. [[CrossRef](#)] [[PubMed](#)]
89. Sun, L.; Zhang, Y.; Cai, T.; Li, X.; Li, N.; Xie, Z.; Yang, F.; You, X. CrrAB regulates PagP-mediated glycerophosphoglycerol palmitoylation in the outer membrane of *Klebsiella pneumoniae*. *J. Lipid Res.* **2022**, *63*, 100251. [[CrossRef](#)] [[PubMed](#)]
90. Inoue, M.; Tsuboi, K.; Okamoto, Y.; Hidaka, M.; Uyama, T.; Tsutsumi, T.; Tanaka, T.; Ueda, N.; Tokumura, A. Peripheral tissue levels and molecular species compositions of N-acyl-phosphatidylethanolamine and its metabolites in mice lacking N-acyl-phosphatidylethanolamine-specific phospholipase D. *J. Biochem.* **2017**, *162*, 449–458. [[CrossRef](#)] [[PubMed](#)]
91. Suda, Y.; Okazaki, F.; Hasegawa, Y.; Adachi, S.; Fukase, K.; Kokubo, S.; Kuramitsu, S.; Kusumoto, S. Structural characterization of neutral and acidic glycolipids from *Thermus thermophilus* HB8. *PLoS ONE* **2012**, *7*, e35067. [[CrossRef](#)] [[PubMed](#)]
92. Nemoto, N.; Kawaguchi, M.; Yura, K.; Shimada, H.; Bessho, Y. PGLN: A newly identified amino phosphoglycolipid species in *Thermus thermophilus* HB8. *Biochem. Biophys. Rep.* **2022**, *32*, 101377. [[CrossRef](#)] [[PubMed](#)]
93. Hirai, Y.; Haque, M.; Yoshida, T.; Yokota, K.; Yasuda, T.; Oguma, K. Unique cholesteryl glucosides in *Helicobacter pylori*: Composition and structural analysis. *J. Bacteriol.* **1995**, *177*, 5327–5333. [[CrossRef](#)] [[PubMed](#)]
94. Nagata, M.; Toyonaga, K.; Ishikawa, E.; Haji, S.; Okahashi, N.; Takahashi, M.; Izumi, Y.; Imamura, A.; Takato, K.; Ishida, H.; et al. *Helicobacter pylori* metabolites exacerbate gastritis through C-type lectin receptors. *J. Exp. Med.* **2021**, *218*, e20200815. [[CrossRef](#)] [[PubMed](#)]
95. Stübs, G.; Fingerle, V.; Zähringer, U.; Schumann, R.R.; Rademann, J.; Schröder, N.W. Acylated cholesteryl galactosides are ubiquitous glycolipid antigens among *Borrelia burgdorferi* sensu lato. *FEMS Immunol. Med. Microbiol.* **2011**, *63*, 140–143. [[CrossRef](#)] [[PubMed](#)]
96. Hove, P.R.; Magunda, F.; de Mello Marques, M.A.; Islam, M.N.; Harton, M.R.; Jackson, M.; Belisle, J.T. Identification and functional analysis of a galactosyltransferase capable of cholesterol glycolipid formation in the Lyme disease spirochete *Borrelia burgdorferi*. *PLoS ONE* **2021**, *16*, e0252214. [[CrossRef](#)] [[PubMed](#)]
97. Mangiarotti, A.; Genovese, D.M.; Naumann, C.A.; Monti, M.R.; Wilke, N. Hopanoids, like sterols, modulate dynamics, compaction, phase segregation and permeability of membranes. *Biochim. Biophys. Acta Biomembr.* **2019**, *1861*, 183060. [[CrossRef](#)] [[PubMed](#)]
98. Malott, R.J.; Wu, C.H.; Lee, T.D.; Hird, T.J.; Dalleska, N.F.; Zlosnik, J.E.; Newman, D.K.; Speert, D.P. Fosmidomycin decreases membrane hopanoids and potentiates the effects of colistin on *Burkholderia multivorans* clinical isolates. *Antimicrob. Agents Chemother.* **2014**, *58*, 5211–5219. [[CrossRef](#)] [[PubMed](#)]
99. Schmerk, C.L.; Welander, P.V.; Hamad, M.A.; Bain, K.L.; Bernards, M.A.; Summons, R.E.; Valvano, M.A. Elucidation of the *Burkholderia cenocepacia* hopanoid biosynthesis pathway uncovers functions for conserved proteins in hopanoid-producing bacteria. *Environ. Microbiol.* **2015**, *17*, 735–750. [[CrossRef](#)] [[PubMed](#)]
100. Renoux, J.M.; Rohmer, M. Prokaryotic triterpenoids. New bacteriohopanetetrol cyclitol ethers from the methylotrophic bacterium *Methylobacterium organophilum*. *Eur. J. Biochem.* **1985**, *151*, 405–410. [[CrossRef](#)] [[PubMed](#)]

101. Garcia Costas, A.M.; Tsukatani, Y.; Rijpstra, W.I.; Schouten, S.; Welander, P.V.; Summons, R.E.; Bryant, D.A. Identification of the bacteriochlorophylls, carotenoids, quinones, lipids, and hopanoids of “Candidatus Chloracidobacterium thermophilum”. *J. Bacteriol.* **2012**, *194*, 1158–1168. [[CrossRef](#)] [[PubMed](#)]
102. Araújo, R.G.; Zavala, N.R.; Castillo-Zacarias, C.; Barocio, M.E.; Hidalgo-Vázquez, E.; Parra-Arroyo, L.; Rodríguez-Hernández, J.A.; Martínez-Prado, M.A.; Sosa-Hernández, J.E.; Martínez-Ruiz, M.; et al. Recent Advances in Prodigiosin as a Bioactive Compound in Nanocomposite Applications. *Molecules* **2022**, *27*, 4982. [[CrossRef](#)] [[PubMed](#)]
103. Stankovic, N.; Radulovic, V.; Petkovic, M.; Vuckovic, I.; Jadranin, M.; Vasiljevic, B.; Nikodinovic-Runic, J. *Streptomyces* sp. JS520 produces exceptionally high quantities of undecylprodigiosin with antibacterial, antioxidative, and UV-protective properties. *Appl. Microbiol. Biotechnol.* **2012**, *96*, 1217–1231. [[CrossRef](#)] [[PubMed](#)]
104. Koyun, M.T.; Sirin, S.; Aslim, B.; Taner, G.; Dolanbay, S.N. Characterization of prodigiosin pigment by *Serratia marcescens* and the evaluation of its bioactivities. *Toxicol. Vitro.* **2022**, *82*, 105368. [[CrossRef](#)] [[PubMed](#)]
105. Klaus, J.R.; Coulon, P.M.L.; Koirala, P.; Seyedsayamdost, M.R.; Déziel, E.; Chandler, J.R. Secondary metabolites from the *Burkholderia pseudomallei* complex: Structure, ecology, and evolution. *J. Ind. Microbiol. Biotechnol.* **2020**, *47*, 877–887. [[CrossRef](#)] [[PubMed](#)]
106. Wood, P.L. Non-targeted lipidomics utilizing constant infusion high resolution ESI mass spectrometry. In *Springer Protocols, Neuromethods: Lipidomics*; Wood, P.L., Ed.; Humana Press: New York, NY, USA, 2017; Volume 125, pp. 13–19; ISBN 978-1-0716-0863-0.
107. Guan, Z.; Johnston, N.C.; Raetz, C.R.H.; Johnson, E.A.; Goldfine, H. Lipid diversity among botulinum neurotoxin-producing clostridia. *Microbiology* **2012**, *158*, 2577–2584. [[CrossRef](#)] [[PubMed](#)]
108. Wood, P.L.; Woltjer, R.L. Electrospray Ionization High Resolution Mass Spectrometry of the Chloride Adducts of Steroids, Mono- and Oligo-saccharides, Xyloglucans, Ceramides, Gangliosides, and Phenols. In *Springer Protocols, Neuromethods: Metabolomics*; Wood, P.L., Ed.; Humana Press: New York, NY, USA, 2021; Volume 159, pp. 69–76; ISBN 978-1-0716-0863-0.
109. Wood, P.L.; Scoggin, K.; Ball, B.A.; Lawrence, L.; Troedsson, M.H.; Squires, E.L. Lipidomics of equine sperm and seminal plasma: Identification of amphiphilic (O-acyl)- ω -hydroxy- fatty acids. *Theriogenology* **2016**, *86*, 1212–1225. [[CrossRef](#)] [[PubMed](#)]
110. Wood, P.L.; Muir, W.; Christmann, U.; Gibbons, P.; Hancock, C.L.; Poole, C.M.; Emery, A.L.; Poovey, J.R.; Scarborough, J.J.; Christopher, J.S.; et al. Lipidomics of chicken egg yolk: High resolution mass spectrometric characterization of nutritional lipid families. *Poult. Sci.* **2021**, *100*, 887–899. [[CrossRef](#)] [[PubMed](#)]
111. Wood, P.L.; Hauther, K.A.; Scarborough, J.H.; Craney, D.J.; Dudzik, B.; Cebak, J.E.; Woltjer, R.L. Human brain lipidomics: Utilities of chloride adducts in flow injection analyses (FIA). *Life* **2021**, *11*, 403. [[CrossRef](#)] [[PubMed](#)]
112. Wood, P.L.; Erol EHoffsis, G.F.; DeBuck, J. Serum Lipidomics of Bovine Paratuberculosis: Disruption of Choline-Containing Glycerophospholipids and Sphingolipids. *Sage Open Med.* **2018**, *6*, 2050312118775302. [[CrossRef](#)] [[PubMed](#)]
113. Laval, F.; Laneelle, M.-A.; Deon, C.; Monsarrat, B.; Daffe, M. Accurate molecular mass detrermination of mycolic acids by MALD-TOF mass spectrometry. *Anal. Chem.* **2001**, *73*, 4537–4544. [[CrossRef](#)] [[PubMed](#)]
114. Schukken, Y.H.; Whitlock, R.H.; Wolfgang, D.; Grohn, Y.; Beaver, A.; VanKessel, J.; Zurakowski, M.; Mitchell, R. Longitudinal data collection of *Mycobacterium avium* subspecies Paratuberculosis infections in dairy herds: The value of precise field data. *Vet. Res.* **2015**, *46*, 65. [[CrossRef](#)] [[PubMed](#)]
115. Aspinall, G.O.; Chatterjee, D.; Brennan, P.J. The variable surface glycolipids of mycobacteria: Structures, synthesis of epitopes, and biological properties. *Adv. Carbohydr. Chem. Biochem.* **1995**, *51*, 169–242. [[PubMed](#)]
116. Hsu, F.F.; Pacheco, S.; Turk, J.; Purdy, G. Structural determination of glycopeptidolipids of *Mycobacterium smegmatis* by high-resolution multiple-stage linear ion-trap mass spectrometry with electrospray ionization. *J. Mass Spectrom.* **2012**, *47*, 1269–1281. [[CrossRef](#)] [[PubMed](#)]
117. Schorey, J.S.; Sweet, L. The mycobacterial glycopeptidolipids: Structure, function, and their role in pathogenesis. *Glycobiology* **2008**, *18*, 832–841. [[CrossRef](#)] [[PubMed](#)]
118. Ryan, E.; Joyce, S.A.; Clarke, D.J. Membrane lipids from gut microbiome-associated bacteria as structural and signalling molecules. *Microbiology* **2023**, *169*, micro001315. [[CrossRef](#)] [[PubMed](#)]
119. Yasuda, S.; Okahashi, N.; Tsugawa, H.; Ogata, Y.; Ikeda, K.; Suda, W.; Arai, H.; Hattori, M.; Arita, M. Elucidation of Gut Microbiota-Associated Lipids Using LC-MS/MS and 16S rRNA Sequence Analyses. *iScience* **2020**, *23*, 101841. [[CrossRef](#)] [[PubMed](#)]
120. Reinink, P.; Buter, J.; Mishra, V.K.; Ishikawa, E.; Cheng, T.Y.; Willemsen, P.T.J.; Porwollik, S.; Brennan, P.J.; Heinz, E.; Mayfield, J.A.; et al. Discovery of *Salmonella* trehalose phospholipids reveals functional convergence with mycobacteria. *J. Exp. Med.* **2019**, *216*, 757–771. [[CrossRef](#)] [[PubMed](#)]
121. Lee, O.Y.; Wu, H.H.; Besra, G.S.; Rothschild, B.M.; Spigelman, M.; Hershkovitz, I.; Bar-Gal, G.K.; Donoghue, H.D.; Minnikin, D.E. Lipid biomarkers provide evolutionary signposts for the oldest known cases of tuberculosis. *Tuberculosis* **2015**, *95* (Suppl. S1), S127–S132. [[CrossRef](#)] [[PubMed](#)]
122. Lee, O.Y.; Wu, H.H.; Donoghue, H.D.; Spigelman, M.; Greenblatt, C.L.; Bull, I.D.; Rothschild, B.M.; Martin, L.D.; Minnikin, D.E.; Besra, G.S. *Mycobacterium tuberculosis* complex lipid virulence factors preserved in the 17,000-year-old skeleton of an extinct bison, *Bison antiquus*. *PLoS ONE* **2012**, *7*, e41923. [[CrossRef](#)] [[PubMed](#)]

123. Masson, M.; Molnár, E.; Donoghue, H.D.; Besra, G.S.; Minnikin, D.E.; Wu, H.H.; Lee, O.Y.; Bull, I.D.; Pálfi, G. Osteological and biomolecular evidence of a 7000-year-old case of hypertrophic pulmonary osteopathy secondary to tuberculosis from neolithic Hungary. *PLoS ONE* **2013**, *8*, e78252. [[CrossRef](#)] [[PubMed](#)]
124. Váradi, O.A.; Rakk, D.; Spekker, O.; Terhes, G.; Urbán, E.; Berthon, W.; Pap, I.; Szikossy, I.; Maixner, F.; Zink, A.; et al. Verification of tuberculosis infection among Vác mummies (18th century CE, Hungary) based on lipid biomarker profiling with a new HPLC-HESI-MS approach. *Tuberculosis* **2021**, *126*, 102037. [[CrossRef](#)] [[PubMed](#)]
125. Spekker, O.; Váradi, O.A.; Szekeres, A.; Jäger, H.Y.; Zink, A.; Berner, M.; Pany-Kucera, D.; Strondl, L.; Klostermann, P.; Samu, L.; et al. A rare case of calvarial tuberculosis from the Avar Age (8th century CE) cemetery of Kaba-Bitózug (Hajdú-Bihar county, Hungary)-Pathogenesis and differential diagnostic aspects. *Tuberculosis* **2022**, *135*, 102226. [[CrossRef](#)] [[PubMed](#)]

Disclaimer/Publisher's Note: The statements, opinions and data contained in all publications are solely those of the individual author(s) and contributor(s) and not of MDPI and/or the editor(s). MDPI and/or the editor(s) disclaim responsibility for any injury to people or property resulting from any ideas, methods, instructions or products referred to in the content.